JOURNAL OF VIROLOGY, Sept. 2007, p. 9878–9890 Vol. 81, No. 18
0022-538X/07/$08.00+0 doi:10.1128/JVI.00562-07

Identification of Nonessential Regions of the nsp2 Replicase Protein of Porcine Reproductive and Respiratory Syndrome Virus Strain VR-2332 for Replication in Cell Culture[▽]

Jun Han, Gongping Liu,† Yue Wang, and Kay S. Faaberg*

Department of Veterinary and Biomedical Sciences, University of Minnesota, Saint Paul, Minnesota 55108

Received 16 March 2007/Accepted 16 May 2007

The nonstructural protein 2 (nsp2) of porcine reproductive and respiratory syndrome virus (PRRSV) is a multidomain protein and has been shown to undergo remarkable genetic variation, primarily in its middle region, while exhibiting high conservation in the N-terminal putative protease domain and the C-terminal predicted transmembrane region. A reverse genetics system of PRRSV North American prototype VR-2332 was developed to explore the importance of different regions of nsp2 for viral replication. A series of mutants with in-frame deletions in the nsp2 coding region were engineered, and infectious viruses were subsequently recovered from transfected cells and further characterized. The results demonstrated that the cysteine protease domain (PL2), the PL2 downstream flanking sequence (amino acids [aa] 181 to 323), and the putative transmembrane domain were critical for replication. In contrast, the segment of nsp2 preceding the PL2 domain (aa 13 to 35) was dispensable for viral replication, and the nsp2 middle hypervariable region (aa 324 to 813) tolerated 100-aa or 200-aa deletions but could not be removed as a whole; the largest deletion was about 400 aa (nsp2Δ324–726). Characterization of the mutants demonstrated that those with small deletions possessed growth kinetics and RNA expression profiles similar to those of the parental virus, while the nsp2Δ324–726 mutant displayed decreased cytolytic activity on MARC-145 cells and did not develop visible plaques. Finally, the utilization of the genetic flexibility of nsp2 to express foreign genes was examined by inserting the gene encoding green fluorescent protein (GFP) in frame into one nsp2 deletion mutant construct. The recombinant virus was viable but impaired and unstable and gradually gained parental growth kinetics by the loss of most of the GFP gene.

Porcine reproductive and respiratory syndrome virus (PRRSV), the etiological agent of porcine reproductive and respiratory syndrome, is an enveloped, positive-stranded RNA virus belonging to the family *Arteriviridae* in the order *Nidovirales* (6) and contains a 15.1- to 15.5-kb-long genome (19, 20). Two genotypes, represented by prototype viruses Lelystad and VR-2332, have been discerned based on a difference in nucleotide sequence by approximately 40%, and are referred to as European strains (EU, or type 1 [Lelystad]) (19) and North American strains (NA or type 2 [VR-2332]) (1, 20). The 5′ two-thirds of the viral genome is occupied by overlapping open reading frames 1a (ORF1a) and 1b, which generate the viral replicase proteins. Polyprotein 1a (pp1a) is encoded by ORF1a, and the synthesis of pp1ab occurs through a ribosomal frameshift at the ORF1a-1b junction (4, 30). These polyproteins are immediately translated upon virus entry and then proteolytically processed by virally encoded proteinases into intermediate precursors and at least 12 mature nonstructural proteins, which appear to be responsible for forming membrane-bound replication complexes, called virus-induced double-membrane vesicles, which are sites for viral RNA synthesis (30).

The processing of pp1a and pp1ab is believed to be mediated by accessory proteinases, located in nsp1 and nsp2, and the main serine proteinase in nsp4, 3C-like proteinase (3CLpro) (40). The catalytic sites of these enzymes and the corresponding cleavage sites are well conserved among arteriviruses (40). Processing of pp1a begins with the N-terminal nsp1, which is automatically cleaved by papain-like cysteine proteases (PCP1α and PCP1β) in PRRSV, while the PCP1α domain is inactive in equine arteritis virus (EAV) (9, 32). Arterivirus nsp2 contains a predicted cysteine proteinase (PL2) in its N terminus that was shown to cleave at the nsp2-nsp3 junction in EAV (33). The 3CLpro is responsible for processing the remainder of ORF1a and ORF1ab into several subunits (nsp3 to -12) (35, 40).

Among the nonstructural proteins, the multidomain protein nsp2 is the largest PRRSV replicative protein and was originally identified as spanning amino acids (aa) 384 to 1363 (nsp2 aa 1 to 981) and then projected to include aa 384 to 1578 (nsp2 aa 1 to 1196) of strain VR-2332 ORF1a through genetic analysis of both *Coronaviridae* and *Arteriviridae* (1, 40). PRRSV nsp2 protein has a similar organization to the arterivirus family member EAV nsp2 counterpart (33, 40). Three major domains could be discerned through the alignment of arterivirus nsp2 proteins: an N-terminal cysteine proteinase domain (PL2), a functionally unspecified middle region, and a hydrophobic transmembrane (TM) region near the C terminus (16, 40). In addition, the exact C-terminal cleavage sites have yet to be determined. PRRSV PL2 is predicted to act on the potential substrates at the nsp2-nsp3 junction and two potential cleavage

* Corresponding author. Mailing address: Virus and Prion Diseases of Livestock Research Unit, National Animal Disease Center, USDA, Agricultural Research Services, Ames, IA. Phone: (515) 663-7259. Fax: (515) 663-7458. E-mail: kay.faaberg@ars.usda.gov.

† Present address: Public Health Laboratories Division, Minnesota Department of Health, Saint Paul, MN 55164.

▽ Published ahead of print on 23 May 2007.

TABLE 1. Oligonucleotide primers used in this study

Primer[a]	Genome position[b]	Sequence[c]
pVR-V7 construction		
T7Leader-VR long/	1–30	5′ ACAT**GCATGC**TTAATACGACTCACTATAGTATGACGTATAG GTGTTGGCTCTATGCCTTGG 3′
/3′-4300	4617–4635	5′ CTGGGCGACCACAGTCCTA 3′
5′-4056-*AscI*/	4055–4080	5′ CTTCTC**GGCGCGCC**CGAATGGGAGT 3′
/3′-7579	7578–7603	5′ TCATCATACCTAGGGCCTGCTCCACG 3′
5′-7579/	7578–7603	5′ CGTGGAGCAGGCCCTAGGTATGATGA 3′
/P32	13293–13310	5′ TGCAGGCGAACGCCTGAG 3′
VR1509/	11938–11958	5′ GTGAGGACTGGGAGGATTACA 3′
/3′end-FL	15405–15411	5′ GTC**TTTAATTAA**CTAG$(T)_{30}$AATTTCG 3′
Construction of GFP recombinant virus, identification of nsp2 mutants, and Northern analysis		
dVR-67U22/	2167–2187	5′ CGCCCGCCACGCGTAATCGACA 3′
/dVR-1307L24	3740–3763	5′ CTGTGCCTGCGGACGGAGCTGATG 3′
/dVR-191L30	GFP	5′ GAGGTGCGGGAATTGGCAAGGACTTTTGAG 3′
dVR-198U34/	GFP	5′ GTCCTTGCCAATTCCCGCACCTCGCGGAACTGTG 3′
dVR-192U30/	GFP	5′ TCAAAAGTCCTTGCCAAAAGTTCAGCCTCG 3′
/dVR-192L30	GFP	5′ CGAGGCTGAACTTTTGGCAAGGACTTTTGA 3′
VR-1051U27/	1051–1077	5′ TCGCCATGCTAACCAATTTGGCTATC 3′
VR-1371U18/	1371–1388	5′ GTGGCGACTGCTACAGTC 3′
/VR-1712L26	1712–1737	5′ GACATCCCAGGGGTCACAGTGACAGT 3′
VR-1824U24/	1824–1847	5′ TTGACCGGCTGGCTGAGGTGATGC 3′
/VR-2430L24	2430–2453	5′ TTGGCATGAGCCCATATTCTTCTC 3′
VR-2812U22/	2812–2833	5′ CCCACCTGAGCCGGCAACACCT 3′
VR-2393U22/	2393–2414	5′ CTAACCGCCGTGCTCTCCAAGT 3′
/VR-3080L37	3080–3116	5′ CCCCGCTCTGCGGCGGTGCTGGGGGAGAGGCCTCATA 3′
VR-3331U26/	3331–3356	5′ GCGCGAGGCATGTGATGCGACTAAGC 3′
/VR-3349L26	3349–3374	5′ GCGTAGCAGGGTCATCAAGCTTAGTC 3′
VR-3667U26/	3667–3692	5′ CTCCGAGGATAAACCGGTAGATGACC 3′
/VR-3847L34	3847–38880	5′ CCGGGATCCTTGGTCAAAGAGCCTTTCAGCTTTT 3′
/VR-4258L31	4258–4279	5′ CCGGGATCCGCCCAGTAACCTGCCAAGAATG 3′
/ORF7 probe	14904–14943	5′ TGGCTGGCCATCCCCCTTCTTTCTCTTCTGCTGCTTGCCG 3′

[a] Forward primers are indicated with a slash (/) after the designator, and reverse primers are preceded by a slash.
[b] Unless otherwise noted, genome position is based on GenBank submission U87392.
[c] Inserted restriction enzyme sites are shown in boldface.

sites have been proposed: 981G/G and 1196G/G/G (1, 40), according to the knowledge obtained from nsp2 of EAV, which prefers G/G dipeptides (33). The function of PRRSV nsp2 in the virus life cycle is currently not known, while EAV nsp2 has been shown to be involved in the generation of double-membrane vesicles together with nsp3 and to serve as a cofactor for the nsp4 protein (31, 37).

Although PRRSV nsp2 possesses potential enzymatic function, it has been shown to be highly heterogeneous and variable. It is well documented that PRRSV nsp2 accounts for the major genetic differences between type 1 and type 2 PRRSV strains, sharing less than 40% similarity at the amino acid level (1, 20). In addition, nsp2 is also the key region for length difference between PRRSV type 1 and type 2 strains. Natural mutations, insertions, or, most notably, deletions are always seen in the middle region or near the N-terminal region of the nsp2 protein in field strains, while the putative PL2 domain, predicted TM domain, as well as the predicted cleavage sites remain well conserved (1, 10, 12, 16, 20, 27, 29).

Reverse genetics provides a very valuable tool to explore the function of viral proteins by targeted gene manipulation. In this study, we explored the genetic flexibility of the PRRSV nsp2 protein and sought to identify critical and nonessential regions in PRRSV VR-2332 nsp2 for viral growth in cell culture. We first developed an infectious clone of type 2 prototype strain VR-2332 and then created mutant constructs by deletion mutagenesis. The mutant viruses were rescued, and their growth properties and RNA synthesis capacities were then evaluated. The results suggested that PRRSV nsp2 contains several nonessential regions for viral replication, while the conserved PL2 domain and transmembrane domain are critical for maintaining nsp2 function. In addition, we assessed the flexible nature of nsp2 by expressing the green fluorescent protein (GFP) in one of the nsp2 deletion mutants. We found that the GFP recombinant virus was viable and induced a typical cytopathic effect (CPE) but displayed an impaired growth rate. In addition, the GFP recombinant virus was unstable and gradually gained fitness, shown by increased growth kinetics through the loss of part of the GFP gene.

MATERIALS AND METHODS

Cells and viral strains. MA-104 cells or cells of a subclone (MARC-145 cells; ATCC CRL-11171), an African green monkey kidney epithelial cell line which supports PRRSV replication, were maintained in Eagle's minimal essential medium (EMEM) (SAFC Biosciences) supplemented with 10% fetal bovine serum at 37°C with 5% CO_2. PRRSV North American prototype strain VR-2332 (U87392) was used as a wild-type (wt) control in all experiments. The derived vaccine strain of VR-2332, Ingelvac PRRS MLV (AF066183), was utilized for genome comparison only.

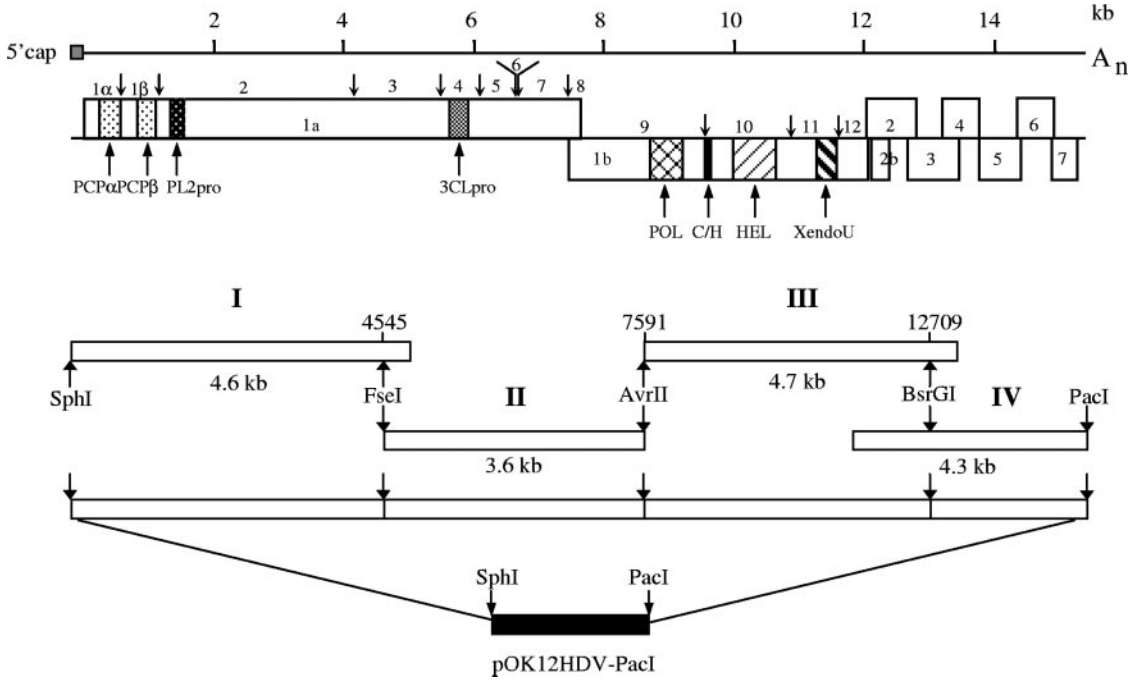

FIG. 1. Assembly of full-length clone of PRRSV strain VR-2332. The 15.4-kb genome was amplified in four sections (I to IV) that incorporated unique restriction enzyme cleavage sites present in viral cDNA (FseI, AvrII, and BsrGI) or added to the PRRSV sequence at the 5′ and 3′ ends by insertion mutagenesis (SphI and PacI). A T7 polymerase promoter and two nontemplated G residues and a T residue preceded the viral sequence. The pOK12 vector was modified to include the above five enzyme restriction sites and an HDV ribozyme downstream of a polyadenosine tail of 50 nucleotides. Signature motifs are identified below ORF1a and -1b, with upwards arrows indicating their placement in the PRRSV genome. Abbreviations: PL2pro, chymotrypsin-like cysteine protease; 3CLpro, serine/3C-like protease; POL, RNA-dependent RNA polymerase; C/H, cysteine/histidine rich; HEL, helicase; XendoU, *Xenopus laevis* homolog poly(U)-specific endoribonuclease.

Construction of PRRSV full-length cDNA clone of VR-2332. cDNA synthesis was performed with the Enhanced avian HS reverse transcription-PCR (RT-PCR) kit (Sigma). Eight PCR primers (Table 1) were used to amplify four overlapping cDNA fragments covering the complete VR-2332 genome (Fig. 1). Each PCR fragment was purified with the QIAEX II gel extraction kit (QIAGEN) and cloned into a pCR2.1-TOPO vector with the TOPO TA cloning kit (Invitrogen). Plasmids representing each fragment were submitted for nucleotide sequence analysis. The QuikChangeMulti site-directed mutagenesis kit (Stratagene) was used to modify all cDNA clones. The fragments with the minimum nucleotide mutations compared to parental VR-2332 sequence (GenBank accession no. U87392) were used to assemble the full-length cDNA, as shown in Fig. 1. In each overlap region, a unique restriction enzyme site was utilized to join flanking fragments. Four digested fragments, representing full-length genomic sequence, were precisely assembled stepwise into a modified low-copy plasmid vector, pOK12HDV-PacI (GenBank accession no. EF486278). The vector was modified to include the hepatitis delta virus (HDV) ribozyme by inserting a 244-bp SmaI-to-SalI fragment containing the HDV antigenome ribozyme and a T7 RNA polymerase terminator sequence from transcription vector 2.0 into the corresponding sites in pOK12 (GenBank accession no. AF223639) (17, 23, 36). The NcoI restriction enzyme site in this 244-bp fragment was replaced with unique SphI and PacI sites by PCR and a linker including FseI, AvrII, and BsrGI restriction sites was then inserted into the site between SphI and PacI by restriction enzyme digestion. Thus, the modified new vector pOK12HDV-PacI contains five unique restriction sites: SphI, FseI, AvrII, BsrGI, and PacI. In the full-length cDNA clone, viral genomic sequence was preceded by the T7 RNA polymerase promoter, two G residues, and a T residue and followed by a poly(A) tail of 50 nucleotides. Assembled clones were propagated in the *Escherichia coli* DH1 cells and then submitted for full-genome nucleotide sequence confirmation (GenBank accession no. DQ217415).

Deletion mutagenesis of PRRSV VR-2332 nsp2. Fragment I (bases 1 to 4545) was digested with SphI and FseI and cloned into the modified pOK12HDV-PacI vector. The subsequent plasmid was named pOK-I. Similarly, fragment II (bases 4545 to 7591) was removed to generate shuttle plasmid pOK-II. To delete VR-2332 nsp2 nucleotides, overlapping extension PCR was performed on pOK-I or pOK-II. One primer pair was used to generate fragment A, and the other primer pair was used to obtain fragment B. Second-round PCR was performed to generate the final full-length deletion fragment with the upstream primer from the first primer set and downstream primer from the second primer pair and the described overlapping fragments A and B as templates. The PCR product was next gel purified, digested with the proper enzymes, and cloned into pOK-I or pOK-II cut with the same enzymes. After confirmation by sequencing, mutated fragment I or II was inserted into the infectious clone backbone to construct the final full-length deletion mutant clone.

To make a recombinant virus expressing GFP, the GFP gene minus the stop codon (714 bp) was inserted into the exact position where the sequence from nsp2 aa 324 to 434 was previously deleted. The insertion of GFP into the nsp2 deletion site was accomplished via three separate PCRs. Two flanking fragments were PCR amplified from pVR-V7-nsp2Δ324–434 by primer sets dVR-67U22/dVR-189L33 and dVR-903U33/dVR-1307L24 and one middle fragment from GFP using primer set dVR-189U33/dVR-903L33. The overlapping extension PCR was completed using all three fragments as templates and primer pair dVR-67U22/dVR-1307L24 to derive the GFP fusion fragment, which was then excised with MluI and EcoRV and cloned back into pOK-I to generate the new plasmid pOK-I-nsp2Δ324–434-GFP. The fragment I-nsp2Δ324–434-GFP was then inserted into the infectious clone backbone as described above to result in full-length clone pVR-V7-nsp2Δ324–434-GFP.

In vitro transcription and transfection. The full-length cDNA clone was linearized by cleavage with PacI. Capped RNA transcripts were produced using the mMESSAGE MACHINE kit (Ambion) with an optimized 2:1 ratio of methylated cap analogue to GTP. The RNA was then purified by the RNeasy mini kit (QIAGEN). RNA was evaluated for quality on 1% native agarose gel and quantified by spectrophotometry at the optical density at 260 nm (OD_{260}). For transfection, a modified procedure was generated based on the approach described by Nielsen et al. (21). MA-104 or MARC-145 cells were seeded onto six-well plates (2×10^5 to 3×10^5 cells/well) in 3 ml of the complete medium EMEM supplemented with 10% fetal bovine serum and then incubated at 37°C in 5% CO_2 for 20 to 24 h until approximately 80% confluent. Three micrograms of in vitro-transcribed RNA and 2 μl of DMRIE-C (Invitrogen) diluted in 1 ml Opti-MEM medium were combined and vortexed briefly. The cells were washed once with Opti-MEM medium and then immediately overlaid with the lipid-

RNA complex solution. After 4 h of exposure to the lipid-RNA complexes, the monolayers were washed and fresh complete medium was added. The transfected cells were monitored daily for appearance of CPE.

Detection of progeny viral RNA. To detect progeny viral RNA, cell culture supernatants from transfected and viral infected cells were harvested. RNA was isolated with QiaAmp viral RNA minikit (QIAGEN). One-step RT-PCR was performed with selected primer pairs (Table 1) to detect parental virus and PRRSV nsp2 mutant viruses.

Immunofluorescence assay. MARC-145 cells grown on coverslips and infected with virus were fixed in 3.7% paraformaldehyde at room temperature for 10 min, permeabilized, and blocked for 20 min with 0.1% Triton X-100–2% bovine serum albumin in phosphate-buffered saline. The cells were incubated for 60 min with PRRSV nucleocapsid protein-specific monoclonal antibody SDOW17 (18) and then stained with goat anti-mouse immunoglobulin G conjugated with Alexa Fluor 568 (Molecular Probes) for another 60 min. The nuclear DNA was stained with DAPI (4′, 6-diamidino-2-phenylindole [Molecular Probes]). The images were collected under an Olympus IX-70 inverted microscope.

Viral growth assays. MA-104 cell monolayers in T-25 flasks were infected with either parental or mutant viruses at a multiplicity of infection (MOI) of 5×10^4 PFU. After 1 h of attachment at room temperature with gentle mixing, the inocula were removed and the monolayers were washed three times with serum-free EMEM. After washing, 7 ml complete medium was added and the flasks were then incubated for up to 5 days at 37°C in 5% CO_2. Samples were collected from medium at different hours postinfection (hpi) and titrated by viral plaque assay. For recombinant virus V7-nsp2Δ324–726 and VR-V7, MARC-145 cells were infected with 10^3 50% tissue culture infective doses ($TCID_{50}$) of the viruses. The virus-infected supernatants were taken every 12 hpi and titrated by an endpoint dilution assay, and the titers were expressed as $TCID_{50}$.

Northern blot analysis. Intracellular RNAs of virus-infected cells were extracted using an RNeasy mini kit (QIAGEN) and electrophoresed (15 μg/sample) on a glyoxal denaturing gel as described previously (20, 39). After RNA transfer to 0.45-μm MagnaGraph nylon transfer membrane (Osmonics), the membrane was probed with an oligonucleotide against ORF7 end labeled with [γ-^{32}P]ATP (Amersham) using polynucleotide kinase (Promega) as described previously (39).

RESULTS

Construction of full-length cDNA clone of VR-2332. Four overlapping genome fragments were amplified from purified strain VR-2332 viral RNA by RT-PCR using the primer pairs indicated (Fig. 1 and Table 1). Each fragment was individually cloned to generate intermediate plasmids pCR-SphI-FseI (segment I), pCR-FseI-AvrII (segment II), pCR-AvrII-BsrGI (segment III), and pCR-BsrGI-PacI (segment IV). The fragments were sequenced, and the mutations were corrected by site-directed mutagenesis. The cDNA clones were then digested with two unique restriction enzymes, as indicated by the clone name. Four fragments were gel purified and ligated stepwise into low-copy vector pOK12HDV-PacI to generate a full-length cDNA clone of PRRSV (pVR-V7). The infectious clone pVR-V7 contains 11 nucleotide and no amino acid changes from wt strain VR-2332, besides those also seen in Ingelvac MLV (Table 2).

Growth properties of recombinant virus VR-V7. The recombinant virus induced typical CPE, characterized by cell clumping, detachment, and lysis at 72 to 96 h posttransfection. At 108 h posttransfection, most of the cells had undergone lysis and detached from the plate (data not shown). In order to rule out the possibility of contamination by wt VR-2332, we sequenced the recombinant virus at passage 3 (P3). The sequencing results confirmed that the exact nucleotide mutations at residues at 7329 and 7554 were detected in virus resulting from pVR-V7 (Table 1). Corresponding mutations were not seen in P3 virus from wt viral RNA transfections (data not shown). Direct immunofluorescence assays were used to detect the expression of PRRSV nucleocapsid protein in infected MARC-145 cells. All cells infected by recombinant virus (P3 and on) as well as wt VR-2332 were positive. Massive nucleolar accumulation of the nucleocapsid protein was readily apparent, as previously reported by Rowland et al. (28; data not shown). The recombinant virus VR-V7 displayed a similar growth rate to wt VR-2332, which also correlated with the viral genomic and subgenomic RNA synthesis. The plaque size of VR-V7 is slightly smaller than that of wt VR-2332 (see Fig. 4B and C).

TABLE 2. Amino acid changes detected in pVR-V7

Region and nucleotide position	ORF aa position	aa change in:		
		VR-2332	pVR-V7	MLV
nsp1a				
309	40	Q	Silent	Q
642	151	P	Silent	P
nsp1b				
1107	306	L	Silent	L
nsp3				
4407	1406	P	Silent	P
4593	1468	Q	Silent	Q
4681	1498	S	**A**	**A**
4866	1559	V	Silent	V
5097	1636	R	Silent	Silent
5247	1686	V	Silent	V
nsp5				
6674	2162	P	**L**	**L**
nsp7				
7329	2380	K	Silent	K
7554	2455	V	Silent	V
nsp11				
11329	3739	G	**A**	**A**
ORF5				
14336	183	G	Silent	G
ORF6				
14404	10	H	Silent	H
14735	121	R	**G**	**G**
14737	121	R	**G**	**G**

[a] Amino acid identity with Ingelvac PRRS MLV is shown in boldface.

Generation and recovery of nsp2 mutant virus. EAV and PRRSV N-terminal ORF1 proteins and their cleavage patterns are depicted in Fig. 2. To determine the functional importance of different regions of nsp2, pVR-V7 fragment I or II was digested with SphI and FseI or FseI and AvrII, respectively, and cloned into the pOK12HDV-PacI adaptor plasmid treated with the same enzymes to generate the shuttle plasmid pOK-I or pOK-II for subsequent nsp2 mutagenesis. The deletions were designed to maintain the ORF1a translational reading frame. Some deletions were based on the deletions seen in the nsp2 region of PRRSV MN184 strains (16), which contained three discontinuous deletions with a total size of 131 aa, compared to strain VR-2332, corresponding to the amino acid positions in PRRSV strain VR-2332 nsp2 of 324 to 434, 486, and 505 to 523, respectively. In order to evaluate the importance of other regions in nsp2, a series of ~100-aa stepwise

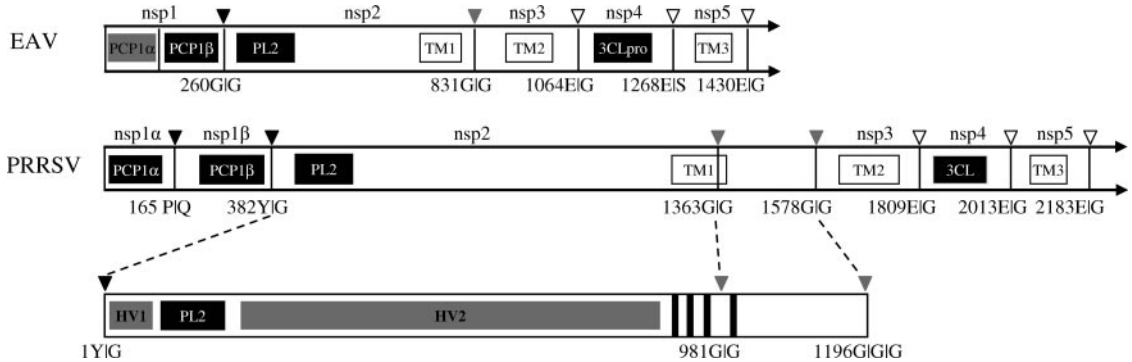

FIG. 2. Schematic of the putative PRRSV nsp2 protein. The organization of the nsp1-to-nsp5 region of PRRSV and EAV is represented schematically. The cleavage sites are labeled by triangles, and the positions are annotated. The putative active enzyme domains are marked by dark boxes, while the inactive PCP1α domain in EAV is boxed gray. The putative TM domains (aa 876 to 898, 911 to 930, 963 to 979, and 989 to 1009) are also shown. Two hypervariable regions (HV) of unknown function are also discerned in the PRRSV nsp2 region.

deletions were created by overlapping PCR (Fig. 3). Each mutated PCR product was digested by the appropriate restriction enzymes and cloned back into pOK-I or pOK-II. After sequence confirmation, mutated fragment I or II was then digested and placed into the infectious clone backbone. After assembly of the full-length cDNAs, at least three clones each were chosen to test downstream viability. The procedures for in vitro transcription and transfection were the same as for VR-V7. Virus-induced CPE was monitored daily after transfection.

Deletions of the PL2 domain and the region immediately downstream are lethal. The PL2 domain is predicted to have a size of about 100 aa (PRRSV Y47 to C147) and is highly conserved among all arteriviruses, especially for the putative active catalytic sites at PRRSV C55 and H124, and has been proposed to be responsible for processing its downstream substrate between nsp2 and nsp3 (16, 33, 40). To test the importance of the PRRSV PL2 domain, an in-frame deletion of nsp2 (Y47 to S180) was engineered and transferred to the infectious clone. The deletion of the PL2 core domain was lethal to the virus, defined as failure to detect extracellular or intracellular replication evidence by RT-PCR or immunostaining after supernatant passage to new cell monolayers and 5 to 6 days subsequent to incubation. Next, we examined the core enzyme domain flanking sequences, which might play a role in maintaining the secondary and tertiary structure of the PL2 domain. For PRRSV nsp2 PL2, its upstream sequence is about 45 aa and highly variable either within or between type 1 and type 2 strains, except for the N-terminal first 7 aa, which are highly conserved and perhaps needed for recognition by PCP1β. Since a natural deletion was seen in MN184 isolates corresponding to positions N324 to P434 in VR-2332, the flanking sequence downstream of PL2 to be examined included residues up to L323. To determine the importance of the regions immediately upstream and downstream of the PL2 domain, either the upstream flanking sequence (A13 to V35 [V7-nsp2Δ13–35]) or downstream sequence (S180 to L323 [V7-nsp2Δ181–323]) was deleted. Transfection of MARC-145 cells with transcript RNA from these constructs indicated that V7-nsp2Δ13–35 resulted in viable virus, while V7-nsp2Δ181–323 was lethal, as confirmed by negative RT-PCR and immunostaining results (data not shown). To rule out the suggestion that the deletion of aa 180 to 323 might have affected the PL2 activity, since the deletion was close to the enzyme domain, another deletion mutant (S241 to L323 [V7-nsp2Δ241–323]) was made. This deletion also turned out to be lethal to virus replication. To negate the possibility that the deletion of these sequences could affect the processing of nsp1, the mutant full-length RNAs were in vitro translated. The results established that nsp1 was correctly processed into nsp1α and nsp1β (data not shown). Taken together, our data revealed that an intact PL2 domain and its immediate downstream flanking sequence were essential for PRRSV replication but the upstream region of nsp2 aa13-35 was dispensable for viral growth.

The hypervariable region of nsp2 aa324–813 tolerated deletions. The region encompassing nsp2 aa150-850, between the PL2 domain and the predicted TM domain, is highly divergent among PRRSV strains and especially between genotypes (1, 20). Several reports have documented that deletions, mutations, and insertions occur in this region (10, 12, 27, 29). We recently reported that nsp2 of MN184 strains contained the largest natural deletions ever found in type 2 field isolates (16). To determine whether the deleted regions seen in the MN184 isolates were required for strain VR-2332 replication, full-length infectious clone pVR-V7 was engineered to lack nsp2 residues D324 through P434 (V7-nsp2Δ324–434) and D324 through A523 (V7-nsp2Δ324–523). Virus-induced CPE was readily detected at 4 to 5 days posttransfection in cells transfected with these nsp2 truncation mutants. Clarified supernatants harvested from MARC-145 cells transfected with VR-V7 nsp2 mutant RNAs were capable of initiating a productive infection in freshly inoculated MARC-145 cells, demonstrating the presence of viable virus. These results indicated that the deletions seen in MN184 strains were also dispensable for strain VR-2332 replication in vitro.

In order to determine whether the entire downstream hypervariable region was dispensable for viral replication, a large deletion mutant (V7-nsp2Δ324–845) from D324 to Q845 was produced but found to be lethal for virus replication. This suggested a detailed stepwise mutagenesis was needed to define the nonessential region boundaries. Four approximately 100-aa or 200-aa deletion constructs were produced as shown in Fig. 4: V7-nsp2Δ543–632 (I543 to R632), V7-nsp2Δ633–726 (I633 to P726), V7-nsp2Δ543–726 (I543 to P726), and V7-

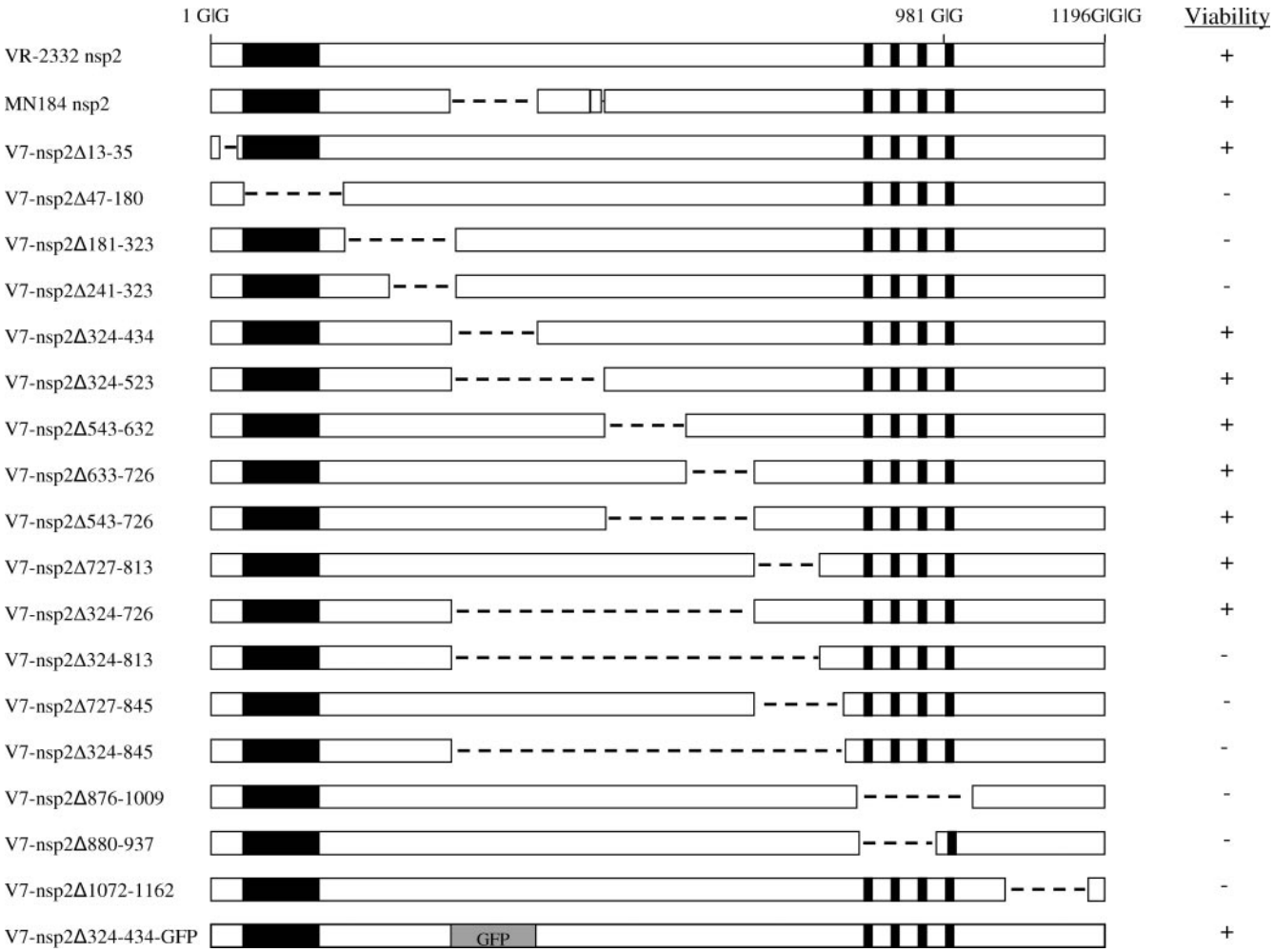

FIG. 3. Construction of strain VR-2332 nsp2 mutants. Mutagenesis was completed to achieve products with in-frame deletions of the nsp2 region by overlapping PCR. The deleted amino acids are shown as a dashed line, and the relative positions are indicated in the individual mutant name. For the purpose of foreign gene expression, the GFP gene was inserted into the position where the region aa 324 to 434 of nsp2 was deleted to generate the mutant V7-nsp2Δ324–434-GFP. The putative enzyme domain and TM region as well as the predicated cleavage sites are shown. The viability for each mutant constructed is shown on the right: +, viable; −, nonviable.

nsp2Δ727–845 (C727 to Q845). The transfection results suggested that only V7-nsp2Δ727–845 produced a nonreplicating PRRSV genome; all others resulted in viable virus. Further bioinformatic analysis suggested that V7-nsp2Δ727–845 might have affected the structure or stability of the juxtaposed hydrophobic domain. Thus, a smaller deletion (C727 to G813 [V7-nsp2Δ727–813]) was also made, and this deletion allowed the rescue of viable virus. Thus, the region of nsp2 aa 324 to 813 did tolerate several 100- to 200-aa deletions. To determine if the whole region could be deleted, two additional deletion constructs (D324 to P726 [V7-nsp2Δ324–726] and D324 to G813 [V7-nsp2Δ324–813]) were generated. The 403-aa deletion (V7-nsp2Δ324–726) allowed viable virus recovery, while construct V7-nsp2Δ324–813 did not. The combined data suggested that VR-2332 nsp2 harbors a large nonessential region for viral replication in cell culture.

The TM region and C-terminal tail are critical for nsp2 function. The carboxyl region of nsp2 is highly conserved among all PRRSV strains and has been predicted to contain three to four putative hydrophobic TM domains (aa 876 to 898, 911 to 930, 963 to 979, and 989 to 1009) (16). This is consistent with the nsp2 counterpart of PRRSV arterivirus family member EAV, which also has TM domains in the respective C termini (33, 40). According to EAV, PL2 prefers G/G dipeptides (33). Thus, a carboxyl-terminal tail was predicted for PRRSV nsp2 that harbors two potential cleavage sites (981G/G and 1196G/G/G) (1, 40). Since the hydrophobic domains are responsible for targeting the nonstructural proteins for intracellular membranes to form viral replication complexes, as demonstrated in EAV (31, 34), a complete deletion (W876 to Q1009 [V7-nsp2Δ876–1009]) of the TM domain was made in an attempt to determine if the hydrophobic region was required for PRRSV replication. The result indicated that the deletion was lethal to the virus. Since a potential cleavage site (981G/G) lay between the third and fourth TM helices (16), a truncated TM (A880 to A937 [V7-nsp2Δ880–937]) was subsequently constructed to maintain the potential cleavage site. However, the deletion

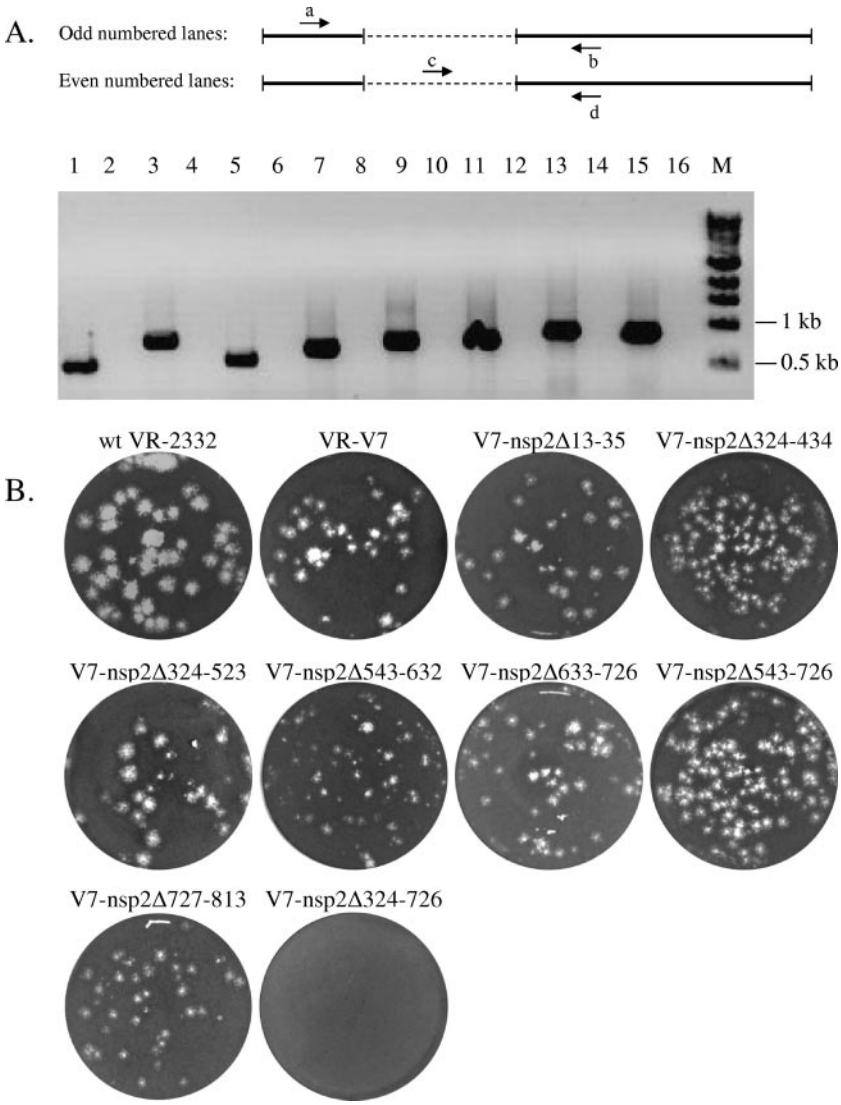

FIG. 4. Characterization of nsp2 small mutants. (A) Identification of viable nsp2 mutant viruses by RT-PCR, as shown in the schematic. One primer set (a/b; indicated for each mutant below) was used to confirm the presence of a mutant virus in the odd-numbered lanes, while another primer set (c/d; indicated for each mutant below) was used to ensure there was no contamination with parental virus in the even-numbered lanes. The detection of mutants nsp2Δ13–35 (VR-1051U27/VR-1712L26 [618 bp]), nsp2Δ324–434 (dVR-67U22/VR-3349L26 [875 bp]), nsp2Δ324–523 (dVR-67U22/VR-3349L26 [608 bp]), nsp2Δ543–632 (VR-2393U32/VR-3349L26 [712 bp]), nsp2Δ633–726 (VR-2812U22/VR-3847L34 [787 bp]), nsp2Δ727–813 (VR-2812U22/VR-3847L34 [808 bp]), nsp2Δ543–726 (VR-2393U32/VR-3847L34 [936 bp]), and nsp2Δ324–726 (dVR-67U22/VR-38474258L31 [904 bp]) is shown in lanes 1, 3, 5, 7, 9, 11, 13, and 15, respectively, and the corresponding detection of wild-type or parental virus contamination is shown in lanes 2 (VR-1371U18/VR-1712L26), 4 (VR-1824U24/VR-2430l24), 6 (VR-2812U24/VR-3349L26), 8 (67U22/VR-3080L37), 10 (VR-3331U26/VR-3847L34), 12 (VR-3667U26/VR-4258L31), 14 (VR-3331U26/VR-3847L34), and 16 (VR-3331U26/VR-4285L31). M refers to a 1-kb DNA ladder (New England Biolabs). (B) Plaque assays for wt VR-2332, VR-V7, and nsp2 mutants were completed in parallel. MARC-145 cells were infected with viruses, and monolayers were stained with crystal violet at 4 days postinfection, while mutant V7-nsp2Δ324–726 was developed 8 to 10 days postinfection. (C) Viral growth curve analysis. MA-104 cells in T-25 flasks were infected with PRRSV nsp2 small deletion mutants and parental virus at an MOI of 10^4 PFU. The cell supernatants were collected for titration analysis by viral plaque assay at different time points. The virus was titrated on MA-104 cells. (D) Northern blot analysis of viral RNA (vRNA) synthesis. MARC-145 cells in T-75 flasks were inoculated with 10^3 $TCID_{50}$ of viruses, and the intracellular RNAs were extracted at 30 hpi. The viral genomic RNA and subgenomic mRNAs 2 to 7 produced by wt VR-2332 (lane 1), VR-V7 (lane 2), V7-nsp2Δ13–35 (lane 3), V7-nsp2Δ324–434 (lane 4), V7-nsp2Δ324–523 (lane 5), V7-nsp2Δ543–632 (lane 6), V7-nsp2Δ633–726 (lane 7), V7-nsp2Δ543–726 (lane 8), V7-nsp2Δ727–813 (lane 9), V7-nsp2Δ324–726 P2-6 (lanes 10 to 14), and mock-infected MARC-145 cell control (lane 15) are shown. The viral RNAs were probed with an oligonucleotide complementary to ORF7.

again resulted in nonviable virus. Similarly, deletion mutagenesis (S1072 to A1162 [V7-nsp2Δ1072–1162]) between the two potential cleavage sites (981G/G and 1196G/G/G) also did not allow virus rescue. Thus, the TM regions and carboxyl-terminal tail appeared to be critical for nsp2 function.

Characterization of nsp2 mutant viruses. First, the possibility of contamination by parental virus was ruled out. Two sets

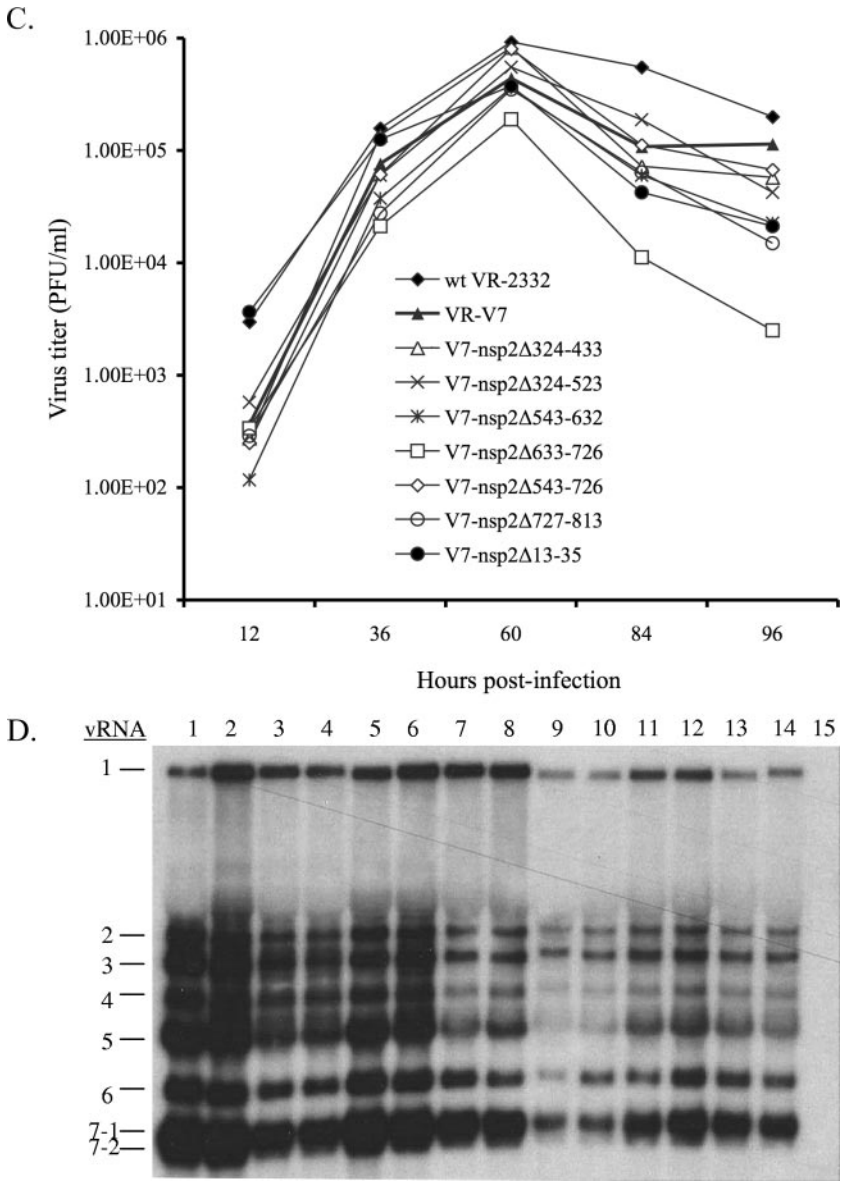

FIG. 4—*Continued.*

of primers were employed to identify each mutant virus: one primer set targeting the sites across the deletion region was to detect the mutant viruses, while the other primer set was used for parental virus detection by targeting the deletion region with one primer. There was no evidence of cross-contamination by VR-V7 virus (Fig. 4A). The nsp2 mutated region integrity of the recombinant viruses was also examined by RT-PCR after four or five passages. All of the viruses maintained the respective engineered deletion with the expected size (Fig. 4A) and had no other mutations within nsp2 (data not shown). The entire genomes of V7-nsp2Δ324–726 P1, P3, and P6 were sequenced to confirm that there were no other compensatory mutations.

To determine the effect of the respective nsp2 deletions on PRRSV growth, the ability to form plaques was first examined. All of the mutants except V7-nsp2Δ324–726 formed viral plaques within 5 days, the sizes of which were either comparable to or smaller than those of the parental virus VR-V7 (Fig. 4B). Further growth curve analysis showed that all of the small deletion mutants had similar growth kinetics to parental VR-V7 recombinant virus, slightly reduced from wt strain VR-2332 (Fig. 4C). To determine if the nsp2 deletions had any effect on viral genomic and subgenomic RNA synthesis, the intracellular RNAs of virus-infected cells at 30 hpi with 10^3 $TCID_{50}$ of P3 viruses were extracted and subjected to Northern blot analysis with a probe against ORF7. Most of these mutants had similar viral RNA expression profiling compared to parental virus VR-V7, except V7-nsp2Δ727–813, which exhibited a decrease in RNA accumulation at 30 h (Fig. 4D, lanes 1 through 9).

Plaque assay results showed that V7-nsp2Δ324–726 could not develop visible plaques even the incubation time was ex-

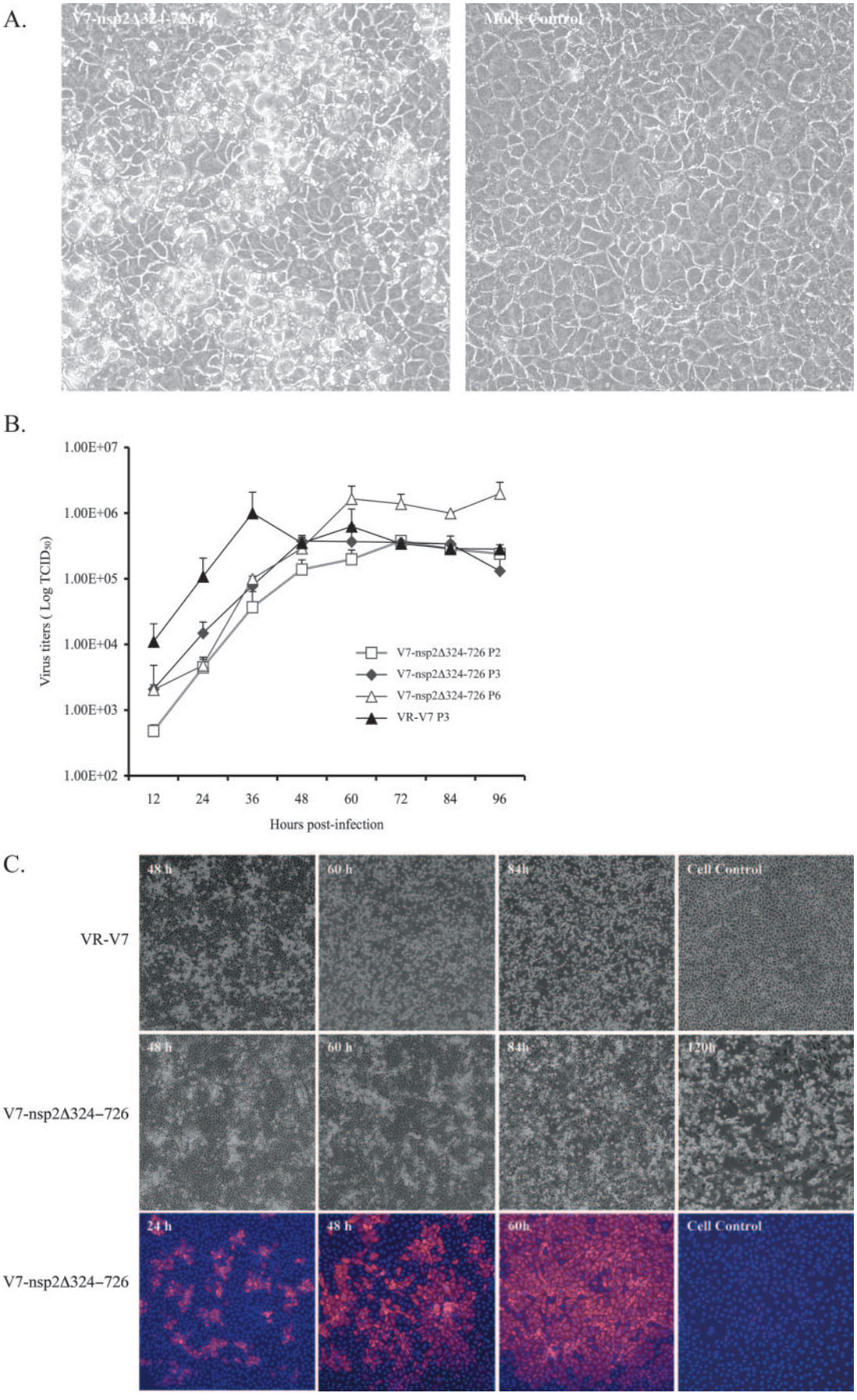

tended to 8 to 10 days (Fig. 4B). Close microscopic investigation of infected cells suggested that the viral infection did cause CPE foci characterized by vacuolization, but the cell walls mostly remained intact and the virus failed to cause complete cell lysis (Fig. 5A). The impaired ability of V7-nsp2Δ324–726 to form visible plaques suggests that some differences exist in the viral replication cycle compared to VR-V7, since plaque development is a consequence of differences in yield, rate of synthesis, and viral release, as well as cytolytic activity (26). On initial transfection of the in vitro-derived transcript RNA, the V7-nsp2Δ324–726 mutant exhibited a 2- to 3-day delay and only sporadic CPE. The virus grew slowly in the first two passages and then reached a titer of around 10^5 $TCID_{50}$/ml at P3 and $10^{5\sim6}$ $TCID_{50}$/ml at P6 (data not shown). To examine the basis of the defect, growth kinetics of V7-nsp2Δ324–726 mutant virus at P2, P3, and P6, monitored by end point dilution assay instead of plaque formation, were determined with an initial inoculum of 10^3 $TCID_{50}$. The V7-nsp2Δ324–726 mutant showed several differences from the parental virus VR-V7. First, V7-nsp2Δ324–726 had a slower growth rate than VR-V7 at early times of infection and exhibited a 12- to 24-h delay in peak titer compared to VR-V7. VR-V7 reached a peak titer around 36 hpi, while V7-nsp2Δ324–726 P6 reached a similar titer at 60 hpi (Fig. 5B). The increase in V7-nsp2Δ324–726 P6 titer at later times in infection may be a consequence of the decrease in cell cytolysis (discussed below). Northern blot analysis, monitoring genomic and subgenomic viral RNA expression levels at 30 hpi for V7-nsp2Δ324–726 P2 to P6 as well as VR-V7, revealed a comparable result (Fig. 4D). Second, V7-nsp2Δ324–726 was impaired in cytolytic activity. The investigation of virus-induced CPE revealed that VR-V7 induced rapid CPE and displayed very rigorous cytolysis, as almost all of the cells were rounded and detached at 55 to 60 hpi, while V7-nsp2Δ324–726 virus caused milder cytolysis (Fig. 5C). V7-nsp2Δ324–726-induced CPE was seen as cell clustering and clumping, with only a portion (30% to 50%) of the cells lysed and detached at both 84 and 120 hpi (Fig. 5C). In order to examine if the decreased cytolysis was due to inefficient infection, an immunofluorescence assay was employed to monitor the infection process at 24, 48, and 60 hpi. There was no apparent defect in cell infection, since more than 90% of the cells were infected by V7-nsp2Δ324–726 at 60 hpi (Fig. 5C), suggesting delayed but typical viral spread. In addition, virus release and the amount of virus produced appeared normal since the mutants reached a comparable titer to VR-V7 at 60 hpi (Fig. 5B). Therefore, the difference in cell viability was most likely due to the decreased cytolytic activity of V7-nsp2Δ324–726. Taken together, it appeared that decreased cytolytic activity played an important role in impairing the ability of V7-nsp2Δ324–726 to form viral plaques (Fig. 4B).

nsp2 is functionally competent with internal insertion of GFP. The identification of several nonessential regions suggests that nsp2 is genetically flexible. To evaluate if nsp2 could accept foreign genes in these nonessential regions, the GFP gene was inserted into one of the viable mutants (V7-nsp2Δ324–434), in frame, in the position where the region of MN184 nsp2 (aa 24 to 434) was deleted compared to that of VR-2332. To test the effect of this nsp2 modification on virus viability, MA-104 cells were transfected with in vitro-transcribed RNA of pVR-V7-nsp2Δ324–434-GFP. Virus-induced CPE was observed 5 to 6 days after transfection. Thus, nsp2 was functionally competent with the internal insertion of the GFP gene, as shown recently for an infectious clone of type 1 PRRSV (11). At passage 2, GFP expression was examined under an inverted fluorescence microscope. GFP was successfully expressed, and the fluorescence was associated with the foci of observed CPE (Fig. 6A and B). Since GFP was expressed as part of the nsp2 protein, the localization of GFP also might reflect the distribution of nsp2 in recombinant virus-infected cells. The visualization of the GFP protein, near the nucleus stained with DAPI, thus suggested that the nsp2 protein was localized in the perinuclear region of the MA-104 cells, a similar distribution pattern to the EAV nsp2 counterpart (Fig. 6C) (24, 34).

Growth, stability, and nsp2-GFP processing of the GFP recombinant virus. To evaluate the growth properties of the GFP recombinant virus, titers were determined from different passages. As shown in Fig. 6D, the GFP insert diminished viral growth, as the GFP recombinant virus grew to very low titers in the first three passages. However, after three passages, the GFP recombinant virus reached a much higher titer of 10^5 $TCID_{50}$/ml, similar to titers of VR-V7. To investigate the basis for the change in growth, the GFP recombinant virus was propagated for five generations. RT-PCR was performed with a primer set (dVR-67U22/dVR-1307L24) amplifying nsp2 across the GFP gene (2 kb). As shown in Fig. 6E, two products were detected in P3 (2 kb and 1.4 kb), and from P4 on, only the smaller 1.4-kb band was detected. The smaller PCR product correlated with the size of the amplicon without GFP. To determine if the virus spontaneously lost the GFP gene and in this manner acquired a growth advantage over the original GFP virus, we determined the nucleotide sequence of the two PCR products. The 2-kb band indeed represented the full-length GFP product, while the 1.4-kb band indicated that splicing had occurred during viral growth, resulting in deletion of all but the first 30 nucleotides of the GFP gene (data not

FIG. 5. In vitro growth properites of V7-nsp2Δ324–726 mutant. (A) Six-well plates were infected with the mutant or left uninfected and incubated for plaque assay. After 9 days, the cells were observed before removal of agarose for virus-induced CPE foci under an inverted microscope. (B) Growth kinetics of V7-nsp2Δ324–726 P2, P3, and P6 as well as VR-V7 P3. The viruses were used to infect MARC-145 cells in T-25 flasks with an MOI of 10^3 $TCID_{50}$. The virus-infected cell supernatants were collected every 12 h and then titrated by using the $TCID_{50}$ assay. (C) Comparison of CPE development by VR-V7 and V7-nsp2Δ324–726 P6. MARC-145 cells in T-25 flasks were infected with VR-V7 P3 and V7-nsp2Δ324–726 P6 at an MOI of 10^3 $TCID_{50}$. Mock-infected cells served as a control. CPE was monitored daily under an inverted microscope (×20). The lower panel indicates the immunfluorescence detection of the viral nucleocapsid protein with monoclonal antibody SDOW-17 in V7-nsp2Δ324–726 P6-infected cells at 24, 48, and 60 hpi, respectively. DAPI was used to stain cell nuclei. The images (×20) were merged by the use of Adobe Photoshop.

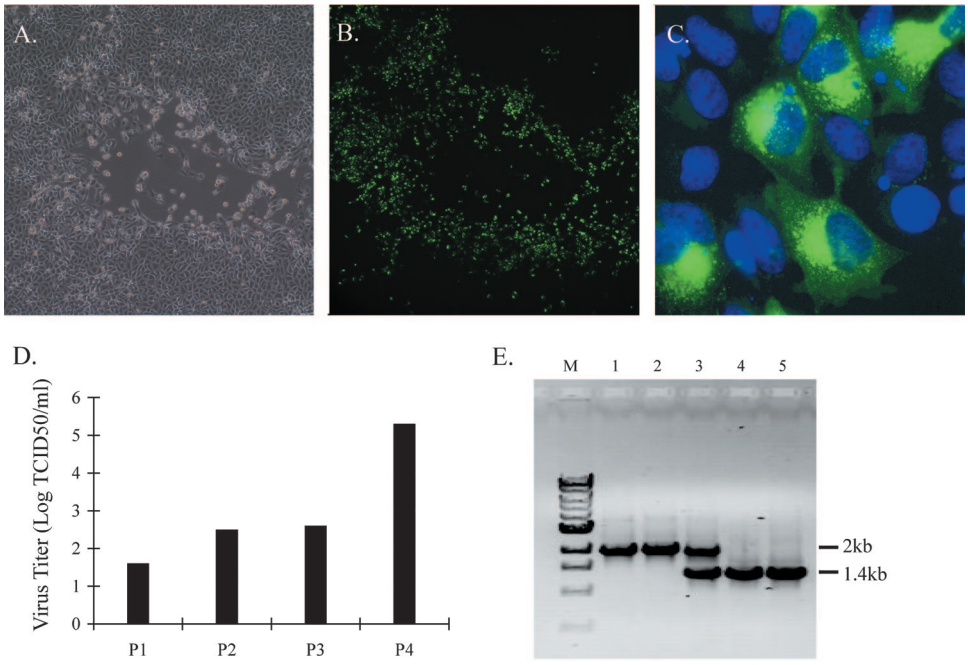

FIG. 6. Utilization of nsp2 to express foreign gene. Viable GFP recombinant virus was generated in MA-104 cells. (A and B) Light (A) and fluorescence (B) (×10) microscopy under the same field showed the fluorescence was associated with the virus-infected foci. (C) A similar field was stained with DAPI (blue) to visualize the cell nucleus (×100). (D) Titration of V7-nsp2Δ324–434-GFP P1 to -5. (E) Stability analysis of the GFP gene by RT-PCR with primers (dVR-67U22/dVR-1307L24) across the GFP gene. Lane M is a 1-kb DNA ladder (New England Biolabs), and lanes 1 to 5 represent V7-nsp2Δ324–434-GFP P1 to -5, respectively.

shown). Green fluorescence was also monitored for P1 to -5 of GFP recombinant virus. The loss of the GFP gene from P4 and on correlated with the RT-PCR results (data not shown). Thus, the increase in the virus titer at P4 and the concomitant loss of fluorescence indicated a gain in replication fitness upon deletion of the GFP gene.

DISCUSSION

In this study, we described the construction of a full-length infectious cDNA clone of North American prototype VR-2332, which differed from the one reported earlier (21). VR-V7 coded for 6 nucleotides (5 aa) of the related vaccine Ingelvac PRRS MLV, whereas the previously published clone was derived independently and possessed 14 nucleotides (9 aa) of Ingelvac PRRS MLV besides 2 additional amino acid mutations in ORF1. More importantly, nine disparate nucleotides located in nsp9 to -12, coding for crucial polymerase and helicase regions, were of wt VR-2332 origin in pVR-V7. We also utilized VR-V7 to examine the genetic flexibility of the nsp2 replicase protein as well as its potential use as an expression vector. PRRSV VR-2332 nsp2 was found to contain several nonessential regions, including aa 13 to 35 before the PL2 domain and aa 324 to 813 in the middle hypervariable section. We also found that the PL2 domain and its immediate downstream sequence as well as the putative TM region were essential for viral replication, suggesting their critical role in maintaining nsp2 function in cell cultures. Finally, we reported the successful insertion of the GFP gene in the nonessential region but found that the recombinant virus was impaired and unstable.

The N terminus of the nidovirus replicase protein has been shown to exhibit considerable genetic variability (13), despite its likely crucial function in viral replication. The variability includes size variation and genetic mutation. In coronaviruses, the N-terminus amino sequence identity varies from less than 30% to over 60% among different groups, with the most variability occurring in the protein domains upstream of the nsp3 orthologs (14, 25). The C terminus of the nsp1 protein of murine hepatitis virus (MHV) and the nsp2 protein of MHV and severe acute respiratory syndrome coronavirus have all been shown dispensable for viral replication (5, 14). Very similarly, broad genetic variation in the N terminus of the PRRSV replicase protein has also been observed, especially in nsp2 and to a lesser degree in nsp1 (1, 10, 12, 16, 20, 27, 29). With the continuing emergence of viral strains during the past 18 years, the nsp2 replicase protein with noted mutations, insertions, and deletions has become a vital region for monitoring the rapid evolution of PRRSV. The earliest report concerning nsp2 variation is from the full genome comparison of North American prototype VR-2332 and European prototype Lelystad (LV) strain (1, 20). The nsp2 of the PRRSV LV strain is 119 aa shorter than that of VR-2332, and the amino acid similarity is under 40%. Since then, several other cases have been reported. The PRRSV type 2 SP strain had an unique insertion of 36 aa relative to the position between aa 813 and 814 of VR-2332 nsp2 (29), and type 2 isolate HB-2(sh)/2002 nsp2 protein contained a unique 12-aa deletion at relative positions aa 466 to 477 (12). Similarly, a 17-aa deletion was identified in the newly identified European-like PRRSV field isolate compared to strain LV (10, 27). Our recent report of

two virulent MN184 strains of North American lineage revealed a further truncated PRRSV nsp2 gene, which is 131 aa shorter than type 2 prototype VR-2332 and contains three discontinuous deletions with a total reduced size of 131 aa, leading to the shortest genome detected to date (15,019 kb) (16). The immense genetic variability of nsp2 protein suggests that the hypervariable regions in nsp2 may play a very limited role for viral replication. Accordingly, we demonstrated this hypothesis was correct in that PRRSV nsp2 contained a vast redundant region, at least for viral replication in cell culture. In contrast, the entire region of the nsp2 protein of EAV was found to be crucial for nsp2/3 processing when placed in a reporter gene construct and expressed in the vaccinia virus T7 system (33). Even small deletions were not tolerated in EAV nsp2 even though it has a similar organization to PRRSV nsp2, possessing a large middle region (500 aa) that separates PL2 from its cleavage site. This may reflect a uniqueness of PRRSV nsp2 among arteriviruses.

We also reported that small deletions in the region of VR-2332 nsp2 aa 324 to 813 did not affect virus viability. However, the deletion of the whole region appeared to be lethal to the virus. We have tried at least five clones (V7-nsp2Δ324–813), but the attempts were not successful. The largest deletion that resulted in viable virus is 402 aa (V7-nsp2Δ324–726). One possible explanation is that there might be a size limit for the middle hypervariable region to maintain the correct folding of functional domain of nsp2, and too large a deletion could interfere with the interaction of PL2 domain and its substrates. Given that regions of nsp2 are highly heterogeneous, the whole region of nsp2 aa 324 to 813 may be dispensable in PRRSV strains besides VR-2332. In other strains, mutations elsewhere in nsp2 might have a compensatory effect in maintaining a proper structure for the nsp2 functional domains.

Although the nsp2 hypervariable region (aa 324 to 726) is dispensable for viral replication, the mutant virus was severely crippled in its ability to form plaques and did not cause complete cell lysis in the final stages of replication. The decreased cytolytic activity appeared to be most likely linked to the defect in plaque formation. Therefore, this may indicate that the long hypervariable region of nsp2 might play an important role in regulating maximal cytotoxicity through an undescribed mechanism. In addition, the nsp2 hypervariable region has been proposed to play an important role against host immune responses. Several reports have documented that the nsp2 hypervariable regions in both type 1 and type 2 PRRSV strains contained several highly immunogenic B-cell epitopes, and the antibodies against these epitopes could be detected as early as 1 week (2, 8, 22). The hypothesis proposed states that linear sequences of the nsp2 protein are strongly antigenic and could serve as decoy epitopes, deflecting the host immune responses away from critical viral proteins (10, 22). Although only speculative, swine inoculation of recombinant viruses with variable length deletions in the nsp2 hypervariable region may lead to a clearer knowledge of the biological function of PRRSV nsp2 in in vivo infection.

PRRSV as a potential viral vector has been investigated previously, but the region of study was mainly focused on the 3′ section of the genome and the size of the insertion, if any, was limited to less than 10 amino acids when fused to viral structural proteins (15). Foreign genes have also been inserted into intergenic regions of PRRSV structural proteins and a transcription regulatory signal prior to the inserted genes was employed to generate subgenomic RNA (38). The exceptional genetic variability of PRRSV nsp2 suggested the likelihood of expressing a large foreign gene as a fusion protein in the viral replicase region. In this study, the identification of nonessential regions in the nsp2 replicase protein provided further guidelines for successful insertion of a foreign gene and increased the possibility of generating viable virus. To test this hypothesis, we inserted the green fluorescent gene into one of the VR-2332 nsp2 deletion mutants (nsp2Δ324–434). The visualization of green fluorescence emitted from infected cells indicated that nsp2 was functionally competent to express a foreign gene in the hypervariable region. However, instability arose in later passages of the GFP mutant, consistent with another recent report (11). In that case, virus instability was seen when the insertion of GFP was attempted in a natural nsp2 deletion position that exists between type 1 and type 2 PRRSV. Many factors could contribute to the instability of GFP expression (3, 7). First of all, the GFP gene is much larger than the length of the deleted sequence. Thus it could potentially exert a strong structural influence on surrounding sequences, especially the nearby PL2 protease domain in its interaction with viral substrates, thereby affecting the efficiency of processing the nsp2 nsp3 cleavage. In addition, the nature of the gene insert and the precise position of insertion might influence virus stability. The stability of the firefly luciferase gene varied strongly on its location in the MHV genome, whereas the *Renilla* luciferase gene was maintained in all of the positions tested (7). Given that PRRSV nsp2 harbors such a large hypervariable region, it is possible that stable insertion is position dependent and that expression of a foreign gene will be successful when insertion is manipulated elsewhere in the coding sequence. Thus, size, insertion position, and the nature of a selected foreign gene appear important when considering nsp2 for gene fusion expression.

In summary, the identification of nonessential regions and successful expression of a foreign gene in the nsp2 region by a reverse genetics approach further extend our knowledge concerning PRRSV nsp2 genetic flexibility. The successful recovery of the shortest self-replicating PRRSV (V7-nsp2Δ324–726 [14.2 kb]) also suggests that certain regions in this RNA virus are more flexible than previously thought. In addition, the attenuation of morphological phenotypes such as plaque appearance and cytolytic activity through modification of the viral replicase gene highlights a promising area for future PRRSV vaccine design.

ACKNOWLEDGMENTS

The United States Department of Agriculture (award 206-01598) and Boehringer Ingelheim Vetmedica, Incorporated, provided funds for this study.

REFERENCES

1. **Allende, R., T. L. Lewis, Z. Lu, D. L. Rock, G. F. Kutish, A. Ali, A. R. Doster, and F. A. Osorio.** 1999. North American and European porcine reproductive and respiratory syndrome viruses differ in non-structural protein coding regions. J. Gen. Virol. **80:**307–315.
2. **Barfoed, A. M., M. Blixenkrone-Moller, M. H. Jensen, A. Botner, and S. Kamstrup.** 2004. DNA vaccination of pigs with open reading frame 1–7 of PRRS virus. Vaccine **22:**3628–3641.
3. **Bosch, B. J., C. A. M. de Haan, and P. J. M. Rottier.** 2004. Coronavirus spike

glycoprotein, extended at the carboxy terminus with green fluorescent protein, is assembly competent. J. Virol. **78:**7369–7378.
4. **Brierley, I.** 1995. Ribosomal frameshifting viral RNAs. J. Gen. Virol. **76:** 1885–1892.
5. **Brockway, S. M., and M. R. Denison.** 2005. Mutagenesis of the murine hepatitis virus nsp1-coding region identifies residues important for protein processing, viral RNA synthesis, and viral replication. Virology **340:**209–223.
6. **Cavanagh, D.** 1997. Nidovirales: a new order comprising Coronaviridae and Arteriviridae. Arch. Virol. **142:**629–633.
7. **de Haan, C. A. M., B. J. Haijema, D. Boss, F. W. H. Heuts, and P. J. M. Rottier.** 2005. Coronaviruses as vectors: stability of foreign gene expression. J. Virol. **79:**12742–12751.
8. **de Lima, M., A. K. Pattnaik, E. F. Flores, and F. A. Osorio.** 2006. Serologic marker candidates identified among B-cell linear epitopes of Nsp2 and structural proteins of a North American strain of porcine reproductive and respiratory syndrome virus. Virology **353:**410–421.
9. **den Boon, J. A., K. S. Faaberg, J. J. M. Meulenberg, A. L. M. Wassenaar, P. G. W. Plagemann, A. E. Gorbalenya, and E. J. Snijder.** 1995. Processing and evolution of the N-terminal region of the arterivirus replicase ORF1a protein: identification of two papainlike cysteine proteases. J. Virol. **69:**4500–4505.
10. **Fang, Y., D. Y. Kim, S. Ropp, P. Steen, J. Christopher-Hennings, E. A. Nelson, and R. R. Rowland.** 2004. Heterogeneity in Nsp2 of European-like porcine reproductive and respiratory syndrome viruses isolated in the United States. Virus Res. **100:**229–235.
11. **Fang, Y., R. R. R. Rowland, M. Roof, J. K. Lunney, J. Christopher-Hennings, and E. A. Nelson.** 2006. A full-length cDNA infectious clone of North American type 1 porcine reproductive and respiratory syndrome virus: expression of green fluorescent protein in the Nsp2 region. J. Virol. **80:**11447–11455.
12. **Gao, Z. Q., X. Guo, and H. C. Yang.** 2004. Genomic characterization of two Chinese isolates of porcine respiratory and reproductive syndrome virus. Arch. Virol. **149:**1341–1351.
13. **Gorbalenya, A. E., L. Enjuanes, J. Ziebuhr, and E. J. Snijder.** 2006. Nidovirales: evolving the largest RNA virus genome. Virus Res. **117:**17–37.
14. **Graham, R. L., A. C. Sims, S. M. Brockway, R. S. Baric, and M. R. Denison.** 2005. The nsp2 replicase proteins of murine hepatitis virus and severe acute respiratory syndrome coronavirus are dispensable for viral replication. J. Virol. **79:**13399–13411.
15. **Groot Bramel-Verheije, M. H., P. J. Rottier, and J. J. Meulenberg.** 2000. Expression of a foreign epitope by porcine reproductive and respiratory syndrome virus. Virology **278:**380–389.
16. **Han, J., Y. Wang, and K. S. Faaberg.** 2006. Complete genome analysis of RFLP 184 isolates of porcine reproductive and respiratory syndrome virus. Virus Res. **122:**175–182.
17. **Johnson, K. L., and L. A. Ball.** 1997. Replication of flock house virus RNAs from primary transcripts made in cells by RNA polymerase II. J. Virol. **71:**3323–3327.
18. **Magar, R., R. Larochelle, S. Dea, C. A. Gagnon, E. A. Nelson, J. Christopher-Hennings, and D. A. Benfield.** 1995. Antigenic comparison of Canadian and US isolates of porcine reproductive and respiratory syndrome virus using monoclonal antibodies to the nucleocapsid protein. Can. J. Vet. Res. **59:** 232–234.
19. **Meulenberg, J. J., M. M. Hulst, E. J. de Meijer, P. L. Moonen, A. den Besten, E. P. de Kluyver, G. Wensvoort, and R. J. Moormann.** 1993. Lelystad virus, the causative agent of porcine epidemic abortion and respiratory syndrome (PEARS), is related to LDV and EAV. Virology **192:**62–72.
20. **Nelsen, C. J., M. P. Murtaugh, and K. S. Faaberg.** 1999. Porcine reproductive and respiratory syndrome virus comparison: divergent evolution on two continents. J. Virol. **73:**270–280.
21. **Nielsen, H. S., G. Liu, J. Nielsen, M. B. Oleksiewicz, A. Bøtner, T. Storgaard, and K. S. Faaberg.** 2003. Generation of an infectious clone of VR-2332, a highly virulent North American-type isolate of porcine reproductive and respiratory syndrome virus. J. Virol. **77:**3702–3711.
22. **Oleksiewicz, M. B., A. Bøtner, P. Toft, P. Normann, and T. Storgaard.** 2001. Epitope mapping porcine reproductive and respiratory syndrome virus by phage display: the nsp2 fragment of the replicase polyprotein contains a cluster of B-cell epitopes. J. Virol. **75:**3277–3290.
23. **Pattnaik, A. K., L. A. Ball, A. W. LeGrone, and G. W. Wertz.** 1992. Infectious defective interfering particles of VSV from transcripts of a cDNA clone. Cell **69:**1011–1020.
24. **Pedersen, K. W., Y. van der Meer, N. Roos, and E. J. Snijder.** 1999. Open reading frame 1a-encoded subunits of the arterivirus replicase induce endoplasmic reticulum-derived double-membrane vesicles which carry the viral replication complex. J. Virol. **73:**2016–2026.
25. **Prentice, E., J. McAuliffe, X. Lu, K. Subbarao, and M. R. Denison.** 2004. Identification and characterization of severe acute respiratory syndrome coronavirus replicase proteins. J. Virol. **78:**9977–9986.
26. **Rapp, F.** 1964. Plaque differentiation and replication of virulent and attenuated strains of measles virus. J. Bacteriol. **88:**1448–1458.
27. **Ropp, S. L., C. E. Mahlum Wees, Y. Fang, E. A. Nelson, K. D. Rossow, M. Bien, B. Arndt, S. Preszler, P. Steen, J. Christopher-Hennings, J. E. Collins, D. A. Benfield, and K. S. Faaberg.** 2004. Characterization of emerging European-like porcine reproductive and respiratory syndrome virus isolates in the United States. J. Virol. **78:**3684–3703.
28. **Rowland, R. R., R. Kervin, C. Kuckleburg, A. Sperlich, and D. A. Benfield.** 1999. The localization of porcine reproductive and respiratory syndrome virus nucleocapsid protein to the nucleolus of infected cells and identification of a potential nucleolar localization signal sequence. Virus Res. **64:**1–12.
29. **Shen, S., J. Kwang, W. Liu, and D. X. Liu.** 2000. Determination of the complete nucleotide sequence of a vaccine strain of porcine reproductive and respiratory syndrome virus and identification of the Nsp2 gene with a unique insertion. Arch. Virol. **145:**871–883.
30. **Snijder, E. J., and J. J. Meulenberg.** 1998. The molecular biology of arteriviruses. J. Gen. Virol. **79:**961–979.
31. **Snijder, E. J., H. van Tol, N. Roos, and K. W. Pedersen.** 2001. Non-structural proteins 2 and 3 interact to modify host cell membranes during the formation of the arterivirus replication complex. J. Gen. Virol. **82:**985–994.
32. **Snijder, E. J., A. L. Wassenaar, and W. J. Spaan.** 1993. Proteolytic processing of the N-terminal region of the equine arteritis virus replicase. Adv. Exp. Med. Biol. **342:**227–232.
33. **Snijder, E. J., A. L. Wassenaar, W. J. Spaan, and A. E. Gorbalenya.** 1995. The arterivirus Nsp2 protease. An unusual cysteine protease with primary structure similarities to both papain-like and chymotrypsin-like proteases. J. Biol. Chem. **270:**16671–16676.
34. **van der Meer, Y., H. van Tol, J. Krijnse Locker, and E. J. Snijder.** 1998. ORF1a-encoded replicase subunits are involved in the membrane association of the arterivirus replication complex. J. Virol. **72:**6689–6698.
35. **van Dinten, L. C., S. Rensen, A. E. Gorbalenya, and E. J. Snijder.** 1999. Proteolytic processing of the open reading frame 1b-encoded part of arterivirus replicase is mediated by nsp4 serine protease and is essential for virus replication. J. Virol. **73:**2027–2037.
36. **Vieira, J., and J. Messing.** 1991. New pUC-derived cloning vectors with different selectable markers and DNA replication origins. Gene **100:**189–194.
37. **Wassenaar, A. L. M., W. J. M. Spaan, A. E. Gorbalenya, and E. J. Snijder.** 1997. Alternative proteolytic processing of the arterivirus replicase ORF1a polyprotein: evidence that NSP2 acts as a cofactor for the NSP4 serine protease. J. Virol. **71:**9313–9322.
38. **Yoo, D., S. K. Welch, C. Lee, and J. G. Calvert.** 2004. Infectious cDNA clones of porcine reproductive and respiratory syndrome virus and their potential as vaccine vectors. Vet. Immunol. Immunopathol. **102:**143–154.
39. **Yuan, S., M. P. Murtaugh, and K. S. Faaberg.** 2000. Heteroclite subgenomic RNAs are produced in porcine reproductive and respiratory syndrome virus infection. Virology **275:**158–169.
40. **Ziebuhr, J., E. J. Snijder, and A. E. Gorbalenya.** 2000. Virus-encoded proteinases and proteolytic processing in the Nidovirales. J. Gen. Virol. **81:**853–879.